Synthetic and Systems Biotechnology 10 (2025) 610–619

Contents lists available at ScienceDirect

Synthetic and Systems Biotechnology

journal homepage: www.keaipublishing.com/en/journals/synthetic-and-systems-biotechnology

Original Research Article

The biosynthesis of trillin 6′-*O*-glucoside: A low-abundance yet pharmacologically active polyphyllin from *Paris polyphylla*

Yaran Suo [1], Shuyu Li [1], Haining Lyu [1], Xin Zhao, Jiale Xing, Xin Chai, Qian Zhang, Chunjin Fu, Chengchao Xu [*], Jingjing Liao [**]

State Key Laboratory for Quality Ensurance and Sustainable Use of Dao-di Herbs, Artemisinin Research Center, and Institute of Chinese Materia Medica, China Academy of Chinese Medical Sciences, Beijing 100700, China

ARTICLE INFO

Keywords:
Paris polyphylla
Tillin 6′-*O*-Glucoside
Anti-bacterial activity
Hemolytic activity
Biosynthesis

ABSTRACT

Natural products from medicinal plants serve as an invaluable resource for drug discovery and development. However, low-abundance natural products are often understudied due to the challenges of obtaining sufficient quantities for pharmacological testing in cells or animals. Additionally, their complex stereochemistry and functional groups make chemical synthesis and purification difficult. In this study, we showcased the power of biosynthetic approaches to explore these underexplored compounds, using the low-abundance polyphyllin trillin 6′-*O*-glucoside from *Paris polyphylla* as an example. We identified two trillin 6′-*O*-glucosyltransferases required for its biosynthesis and successfully reconstructed the entire pathway in *Nicotiana benthamiana*. We demonstrated that trillin 6′-*O*-glucoside exhibits anti-bacterial activity comparable to major polyphyllins like polyphyllins I, II, and VII. Notably, it also showed much lower hemolytic activity, a common side effect of those major polyphyllins. Together, our study underscores the advantages of employing biosynthetic approaches to explore natural products that exist in low or trace abundances yet possess equally important pharmacological activities.

1. Introduction

Paris polyphylla is a medicinal plant that has a significant history in traditional Chinese medicine [1]. The major ingredients responsible for the pharmacological effects of *P. polyphylla* are polyphyllins, a class of glycosylated steroidal saponins [2]. To date, over 200 steroidal saponins have been isolated from *P. polyphylla* [3–6]. Among them, the pharmacological activities of polyphyllins with high abundance, such as polyphyllins I, II, and VII, have been examined [7]. These polyphyllins demonstrate a broad spectrum of biological activities, including antimicrobial and antiviral properties [8,9], suppression of cancer cell migration and invasion [10–14], as well as neuroprotective [15] and anti-inflammatory effects [16].

However, the polyphyllins with low-abundance are more challenging to study and are frequently overlooked. This is primarily due to the limited availability from native plants for experiments evaluating their pharmacological activities in cells or animals. Moreover, chemical synthesis of polyphyllins with specific sugar moieties in large quantities remains difficult [17]. Fortunately, the advent of synthetic biology offers a solution to this issue: first by elucidating the biosynthetic pathway of those rare polyphyllins, followed by reconstituting their production in a heterologous system [18].

Recent studies have significantly advanced our understanding of the biosynthetic pathways of polyphyllins in medicinal plants. Cholesterol serves as the common precursor upon which the cytochrome P450 enzymes catalyze the formation of the 5,6-spiroketal moiety, resulting the synthesis of diosgenin [19–22]. Diosgenin can potentially be transformed into pennogenin through an enzymatic process likely involving another cytochrome P450 [23]. The uridine diphosphate (UDP)-dependent glycosyltransferases (UGTs) add diverse sugar moieties, such glucose, rhamnose, arabinose, and xylose to diosgenin and pennogenin, leading to the synthesis polyphyllins [24–27]. Many efforts have greatly enhanced our knowledge of the biosynthetic pathways of major polyphyllins in *P. polyphylla*, such as polyphyllins I, II, and VII [23,25]. For

Peer review under the responsibility of Editorial Board of Synthetic and Systems Biotechnology.
* Corresponding author.
** Corresponding author
E-mail addresses: ccxu@icmm.ac.cn (C. Xu), jjliao@icmm.ac.cn (J. Liao).
[1] These authors contributed equally.

https://doi.org/10.1016/j.synbio.2025.02.013
Received 19 January 2025; Received in revised form 13 February 2025; Accepted 19 February 2025
Available online 28 February 2025

instance, the biosynthetic pathway of polyphyllin I has been partially resolved in *P. polyphylla*. While the UDP-glucosyltransferase and UDP-rhamnosyltransferase that participate in polyphyllin I have been reported, the final UDP-arabinosyltransferase is missing [25]. By contrast, the biosynthetic pathway of low-abundance polyphyllins remains largely unexplored. These polyphyllins are likely either direct intermediates of the major polyphyllins or off-pathway products originating from the intermediates catalyzed by competing UGTs not belonging to the pathway.

It is important to note that those low-abundance polyphyllins could potentially exhibit comparable or even better pharmacological activities to the major polyphyllins, albeit often with relatively less sugar moieties. In this study, we demonstrated how biosynthetic approaches are adept at exploring these types of largely uncharted natural products, using a very low-abundance polyphyllin as an example. Trillin 6′-*O*-glucoside is a polyphyllin identified in the rhizomes of *P. polyphylla*. In a prior study, it was demonstrated that only 3.9 mg of trillin 6′-*O*-glucoside could be obtained from 10 kg of dried rhizomes [6]. Chemically synthesized trillin 6′-*O*-glucoside exhibits antifungal activities [28]. Using the biosynthetic approaches, we identified the *Pp*UGTs required for the biosynthesis of trillin 6′-*O*-glucoside and reconstituted the entire pathway in *N. benthamiana*. We demonstrated the anti-microbial activities of trillin 6′-*O*-glucoside against pathogens, which was comparable to major polyphyllins like polyphyllins I, II, and VII. Importantly, trillin 6′-*O*-glucoside displayed much lower hemolytic activity, a common side effect associated with those major polyphyllins. Taken together, our study highlights the advantages of using biosynthetic approaches to explore natural products that are present in low or trace abundances yet possess equally important pharmacological activities.

2. Materials and methods

2.1. Plant materials and chemicals

N. benthamiana plants were grown in a greenhouse following a previously established protocol at the Institute of Chinese Materia Medica, China Academy of Chinese Medical Sciences [29]. The temperature was 25 °C and the relative humidity was 60 %. *P. polyphylla* Smith var. *yunnanensis* samples were obtained from Yunnan, China. Diosgenin, trillin and UDP-glucose were purchased from Better Health For People Ltd. (Beijing, China). All other chemicals were sourced from Sigma-Aldrich (St. Louis, MO, USA).

2.2. RNA isolation and real-time PCR assay

Total RNA was extracted from *P. polyphylla* following the manufacturer's instructions (Eastep™ Super Total RNA Extraction Kit, Promega Biotech Co., Ltd., Beijing, China). PrimeScrip RT Master Mix (Perfect Real Time) (Takara Biomedical Technology Co., Ltd., Beijing, China) was used to synthesized first-strand cDNA. Real-time PCR was conducted on a QuantStudio 5 Real-time PCR Instrument (Thermo Fisher Scientific, Waltham, USA) (with TB Green Premix Ex *Taq*II (Tli RNaseH Plus, Takara Biomedical Technology Co., Ltd., Beijing, China). Primers for real-time PCR are detailed in the Supplementary Table S1. As a housekeeping gene that is routinely used, β-actin was selected as the reference gene [24,25,30], and relative transcript levels were calculated using the $2^{-\Delta\Delta Ct}$ method. Each real-time PCR assay included three biological replicates and three independent technical replicates.

2.3. Transcriptomic analysis and PpUGTs characterization in P. polyphylla

The Hidden Markov Model (HMM) profile for UGTs (PF00201) was retrieved from Pfam (https://pfam.xfam.org/). Candidate *Pp*UGTs were identified using the HMM file and TBtools-II software [31], based on the *P. polyphylla* transcriptome dataset (SRR9118497). Redundant sequences were removed, and only amino acid lengths between 400 and 600 were further investigated. Candidate genes with an FPKM value (Fragments Per Kilobase of exon per Million mapped reads) of 0 were excluded. UGT sequences of *Arabidopsis thaliana* were obtained from TAIR (https://www.arabidopsis.org/index.jsp). Phylogenetic analysis was performed using ClustalW for sequence alignment, and a phylogenetic tree was constructed using MEGA 7.0 software with the Neighbor-Joining algorithm and 2000 bootstrap replicates. And the candidate *Pp*UGTs were classified into the known subfamilies. The UGTs (*Pp*UGT91AH4 and *Pp*UGT91AH5) were named in accordance with the UGT Nomenclature Committee (https://labs.wsu.edu/ugt).

2.4. Recombinant protein expression and purification

The coding sequences of candidate genes were synthesized by Sangon Biotech Co., Ltd. (Shanghai, China), and subcloned into the pGEX-4T-1 vector using the ClonExpress® Ultra One-Step Cloning Kit (Vazyme Biotech, Jiangsu, China). The constructs were subsequently transformed into the *Escherichia coli* (*E. coli*) strain BL21 (DE3). Gene-specific primers were listed in the Supplementary Table S1. The colonies harboring the recombinant plasmid were cultured in liquid Luria Broth (LB) medium containing 100 μg/mL of ampicillin at 37 °C. When the optical density (OD_{600}) reached 0.6–0.8, 0.25 mM isopropyl β-D-1-thiogalactopyranoside (IPTG) was added to induce protein expression, and the culture was incubated at 16 °C for 18 h. Cell pellets were harvested by centrifugation at 5,000 *g* for 15 min at 4 °C, resuspended in lysis buffer (2.7 mM KCl, 10 mM Na_2HPO_4, 1.8 mM KH_2PO_4, 140 mM NaCl, pH 7.4), and lysed by sonication. The lysate was centrifuged at 12,000 rpm for 30 min at 4 °C, and the supernatant was filtered through a 0.22 μm membrane. Recombinant proteins were purified using a glutathione (GST) agarose affinity column (Smart-Lifesciences, Changzhou, China). Protein concentration was determined using a BCA Protein Assay Kit (Thermo Fisher Scientific, Waltham, USA) and purity was assessed by sodium dodecyl sulfate-polyacrylamide gel electrophoresis (SDS-PAGE).

2.5. Enzyme activity and biochemical properties analysis

Enzyme activity assay and product analysis were conducted following the previously described method [32], using recombinant UGT proteins fused with GST tag. The *in vitro* reaction mixture (100 μL) contained 50 mM/L Tris-HCl (pH 8.0), 1 mM $MgCl_2$, 50 μM sugar acceptor, 5 mM UDP-glucose (UDP-rhamnose or UDP-arabinose) and 1 μg purified proteins. The mixture was incubated at 37 °C for 2 h, and the reaction products were extracted with ethyl acetate, dried under vacuum, and resuspended in 100 μL methanol. Substrates and products were analyzed using an Agilent 6546 LC/Q-TOF mass spectrometer equipped with an ACQUITY UPLC BEH C18 column (100 mm × 2.1 mm, 1.7 μm). The mobile phase consisted of 0.1 % formic acid in water (A) and acetonitrile (B), with a gradient elution program. The pH and temperature were optimized. Kinetic parameters (K_m and k_{cat}) were determined using varying concentrations of trillin, and data were analyzed using GraphPad Prism 8.0.

2.6. Transient expression of PpUGTs in N. benthamiana

The coding sequences of *Pp*UGT91AH4 and *Pp*UGT91AH5 were cloned into the pEAQ-HT-GFP vector. Primers used for recombinant plasmids construction were listed in Supplementary Table S1. *Agrobacterium tumefaciens* containing recombinant plasmids were cultured in liquid LB medium (50 μg/mL kanamycin and 25 μg/mL rifampicin) at 28 °C and shaken (180 rpm) for 24 h. Bacterial cultures were centrifuged at 5,000×*g* for 15 min and resuspended in MMA buffer (consisting of 10 mM 2-(*N*-Morpholino)ethanesulfonic acid (MES) with KOH of pH 5.6, 10 mM magnesium chloride, 100 μM acetosyringone and 0.01 % Triton X-100). 6-Week-old *N. benthamiana* plants were kept in the dark for 3 h

before infiltration. pEAQ-HT-GFP vector served as the empty vector control in this experiment. For the *Pp*UGTs functional assay, 1 mg/mL trillin was infiltrated into the leaves 4 days post-infiltration. Leaf samples (100 mg) were collected 5 days after infiltration. In synthesis experiments, equal volumes of all *Agrobacterium* cultures were combined and co-infiltrated, and leaf samples collected 5 days after infiltration. Metabolites were extracted and analyzed following the method described in earlier studies [32].

2.7. Product purification and structure determination

The reactions were performed in 250 mL of the reaction buffer (15 mg trillin and 1.5 L of cell lysates) at 37 °C for 2 h. Reactions were extracted by ethyl acetate and concentrated with a rotary evaporator. It was dissolved in 6 mL methanol for subsequent analysis. For structural identification, glycosides were purified using a preparative Ultimate 3000 HPLC (Thermo Fisher Scientific, Waltham, USA) equipped with Ultimate C18 column. Ultimate C18 column. Optima™ LC/MS solvents (Fisher Chemical) were used, with isocratic elution at a flow rate of 3 mL/min, consisting of 30 % solvent B (acetonitrile) in solvent A (water) (v/v) for 20 min. The purified glycosylated products were dissolved in dimethyl Chloroform-d and analyzed using an AVANCE III 600 MHz NMR spectrometer (nuclear magnetic resonance spectroscopy). Structural characterization was conducted with ^{1}H, ^{13}C NMR, correlation spectroscopy (COSY), heteronuclear multiple bond correlation (HMBC) and heteronuclear single quantum coherence (HSQC). All experiments were performed with using standard Bruker pulse sequences and analyzed using Bruker Topspin 4.0.6.

2.8. Trillin 6′-*O*-glucoside content analysis

The content of trillin 6′-*O*-glucoside was analyzed following previously described methods [32] with Waters ACQUITY H-class plus UPLC System with an ACQUITY UPLC BEH C18 (2.1 mm × 100 mm, 1.7 μm). The mobile phases consisted of water (0.1 % formic acid) (A) and methanol (B). The elution gradient was as follows: 40 % B, for 0–2 min; 40 %–99 % B, for 2–5 min; 99 % B, for 5–7 min; 99 %–40 % B, for 7–7.1 min; 40 % B, for 7.1–10 min with the flow rate of 0.3 mL/min. The optimized parameters for trillin 6′-*O*-glucoside included a multiple reaction monitoring (MRM) transition of 761.0/365.0 and a collision energy (CE) of 59 V in positive ion mode. The calibration curve for trillin 6′-*O*-glucoside was obtained with the equation: $y = 276.075\chi - 21.4836$ ($R^2 = 0.998920$).

2.9. Anti-bacterial activity assay

Bacterial culture and anti-bacterial activity assays were conducted following the literature with minor modifications [33,34]. The study included three Gram-positive (*Staphylococcus aureus*, *Peptostreptococcus anaerobius* and *Clostridium difficile*) and two Gram-negative bacteria (*Campylobacter jejuni* and *Veillonella parvula*), all maintained in the laboratory. *S. aureus* and *C. jejuni* were cultured on hydrolyzed casein (MH) agar plates with 5 % sterile defatted sheep blood (Thermo Fisher Scientific, Waltham, USA), at 37 °C under microaerophilic conditions. *C. difficile*, *V. parvula* and *P. anaerobius* were grown on trypsin soy agar (TSA) agar plates containing 5 % sterile defatted sheep blood under anaerobic condition at the same temperature. Anaerobic conditions were established using Anaerogen (AN0035; Thermo Fisher Scientific, Waltham, MA). Anti-bacterial activity was assessed using the microbroth dilution method, with final bacterial concentrations set at approximately 10^9 CFU/mL. Absorbance (600 nm) was determined using EnVision 2105 multimode plate reader (PerkinElmer, USA). DMSO served as negative control, and microbial suspension was blank controls. Heatmaps illustrated using GraphPad Prism 8.0. All experiments were performed in three independent replicates. For scanning electron microscopy (SEM), samples exposed to trillin 6′-*O*-glucoside (1 μM) or DMSO (negative control) were collected and then fixed in 2.5 % glutaraldehyde at 4 °C overnight. SEM studies were performed using a scanning electron microscope (Hitachi SU-8010, Tokyo, Japan).

2.10. Hemolytic assay

The hemolytic activity of the compounds was evaluated on erythrocytes with minor modifications to previously described methods [35,36]. Sheep erythrocytes (10 mL; Laboratoire Quelab, Montréal, QC, Canada) were collected and centrifuged at 3000 rpm for 20 min. The plasma was removed, and the cells were washed with physiological saline for 3–4 times. The washed erythrocytes were then diluted with physiological saline to 10 % red blood cell suspension. 1 % red blood cell suspension was further used for hemolysis assay. Compounds were evaluated at concentrations between 0 and 2 g/mL (physiological saline was negative control; Triton X-100 was positive controls). After gentle mixing, the samples were incubated at 37 °C for 3 h, and centrifugation at 3,500 rpm for 5 min. 100 μL supernatant was transferred to a 96-well plate, the absorbance (A) was measured using an EnVision 2105 multimode plate reader (PerkinElmer, USA) at 570 nm. The hemolysis rate was calculated as following: Hemolysis rate = $((A_n - A_{nc}) * 100\ \%)/(A_{pc} - A_{nc}) \cdot A_n$, the absorbance of experimental group, A_{nc}, the absorbance of negative control, and A_{pc}, the absorbance of the positive control. Experiments were performed in triplicate, and the median effective concentration (EC_{50}) values were determined based on the concentration causing 100 % hemolysis. Data were expressed as mean ± standard deviation.

3. Results

3.1. Identification PpUGTs potentially involved in trillin 6′-*O*-glucoside biosynthesis

Based on the chemical structure of trillin 6′-*O*-glucoside, it should be synthesized by two glycosyltransferases from diosgenin, with trillin serving as the mono-glycosylated intermediate. Since the trillin synthases have been reported, the key step in elucidating the biosynthetic pathway of trillin 6′-*O*-glucoside lies in discovering the second glycosyltransferase. We speculated that the low levels of trillin 6′-*O*-glucoside could be attributed to two potential reasons: either it was a byproduct generated another UGT due to its promiscuous glucosyltransferase activity, or there exists a dedicated glucosyltransferase that had limited access to trillin. To identify the *Pp*UGTs required for trillin 6′-*O*-glucoside biosynthesis, we employed an *in vitro* enzyme assay. This assay was designed to evaluate the glucosyltransferase activity of recombinantly expressed *Pp*UGTs using trillin and UDP-glucose as substrates in the reaction mixture.

To select the candidate *Pp*UGTs, we re-analyzed the previously published transcriptome data of *P. polyphylla* (SRR9118497) available at the National Center for Biotechnology Information (NCBI). Since trillin 6′-*O*-glucoside was detected only in trace amounts, we hypothesized that the expression levels of candidate *Pp*UGTs could not serve as reliable selection criteria. Consequently, we focused on *Pp*UGTs belonging to the *Pp*UGT73, *Pp*UGT80, and *Pp*UGT91 subfamilies, as these groups include members with documented glucosyltransferase activities (Fig. 1A). After excluding those *Pp*UGTs with other reported functions [25,26,32], 13 candidates were selected (Supplementary Fig. S1), cloned into the pGEX-4T-1 vector, and recombinantly expressed in *E. coli* (Supplementary Fig. S2). Furthermore, a GST tag was incorporated to facilitate purification. Among the tested *Pp*UGTs, we identified two candidates capable of using utilize UDP-glucose to modify trillin, yielding a new, more hydrophilic product that eluted at 5 min in liquid chromatography (Fig. 1B). To determine whether these two *Pp*UGTs exhibited similar activities in plants, we used the transient gene expression in *N. benthamiana* leaves. pEAQ-HT-GFP served as empty vector. The transformed *A. tumefaciens* strains were then infiltrated into

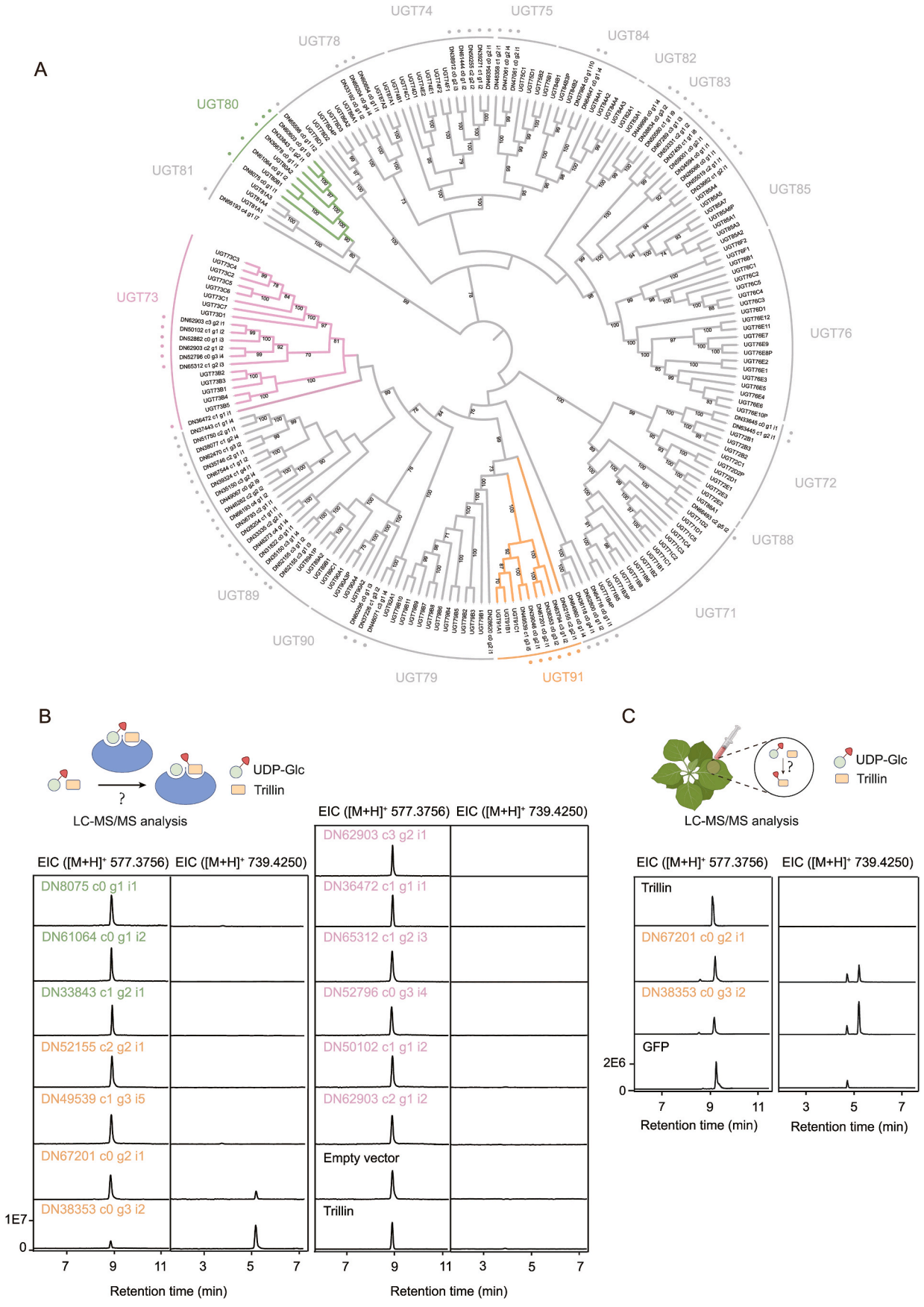

(caption on next page)

Fig. 1. Identification of *Pp*UGTs potentially involved in the biosynthesis of trillin 6′-*O*-glucoside (A) Phylogenetic analysis of *Pp*UGTs. The UGTs from *Arabidopsis thaliana* are used to annotate *Pp*UGTs. Candidate *Pp*UGTs with an FPKM value greater than 0 are selected and marked with circles. *Pp*UGTs belonging to the *Pp*UGT73, *Pp*UGT80, and *Pp*UGT91 subfamilies are highlighted with pink, green, orange circles, respectively. Other *Pp*UGTs are labelled with gray circles. (B) *In vitro* enzyme activity assay of *Pp*UGTs. Candidate *Pp*UGTs were recombinantly expressed and purified. The enzyme activity is tested by incubating trillin and UDP-glucose in the reaction mixture. The products are analyzed by LC-MS and identified as $[M + H]^+$ ions. Lysates prepared from *E. coli* with the empty vector are used as the negative control. (C) Testing the enzyme activity of *Pp*UGTs in *N. benthamiana*. Extracts from *N. benthamiana* leaves were analyzed by LC-MS, and $[M + H]^+$ ions were identified. Leaves infiltrated with the pEAQ-HT-GFP vector served as the negative control.

N. benthamiana leaves. Four days after the initial infiltration, trillin was supplied through a second infiltration to serve as the substrate. UDP-glucose was not added, as *N. benthamiana* leaves contain endogenous UDP-glucose. The leaves were harvested five days after the initial infiltration for metabolic profiling. As expected, these two *Pp*UGTs produced the same new products in *N. benthamiana* leaves (Fig. 1C). Phylogenetic analysis showed that these two *Pp*UGTs belonged to the UGT91 subfamily and were designated as *Pp*UGT91AH4 and *Pp*UGT91AH5, respectively (Fig. 1A). Additionally, we verified the expression of *PpUGT91AH4* and *PpUGT91AH5* in the rhizomes and leaves, respectively (Supplementary Fig. S3).

Taken together, we identified two *Pp*UGTs from *P. polyphylla* that are capable of glycosylating trillin, utilizing UDP-glucose as the sugar donor.

3.2. Structural determination of the new product catalyzed by PpUGT91AH4 and PpUGT91AH5

Because trillin 6′-*O*-glucoside is not commercially available, we aimed to elucidate the structure of the new product catalyzed by *Pp*UGT91AH4 or *Pp*UGT91AH5 and verify whether it is trillin 6′-*O*-glucoside. LC-MS analysis revealed that the *m/z* of the $[M + H]^+$ ion of the new product was 739.4250, which corresponds exactly to the molecular weight of a glycosylated trillin. Analysis of the fragmentation

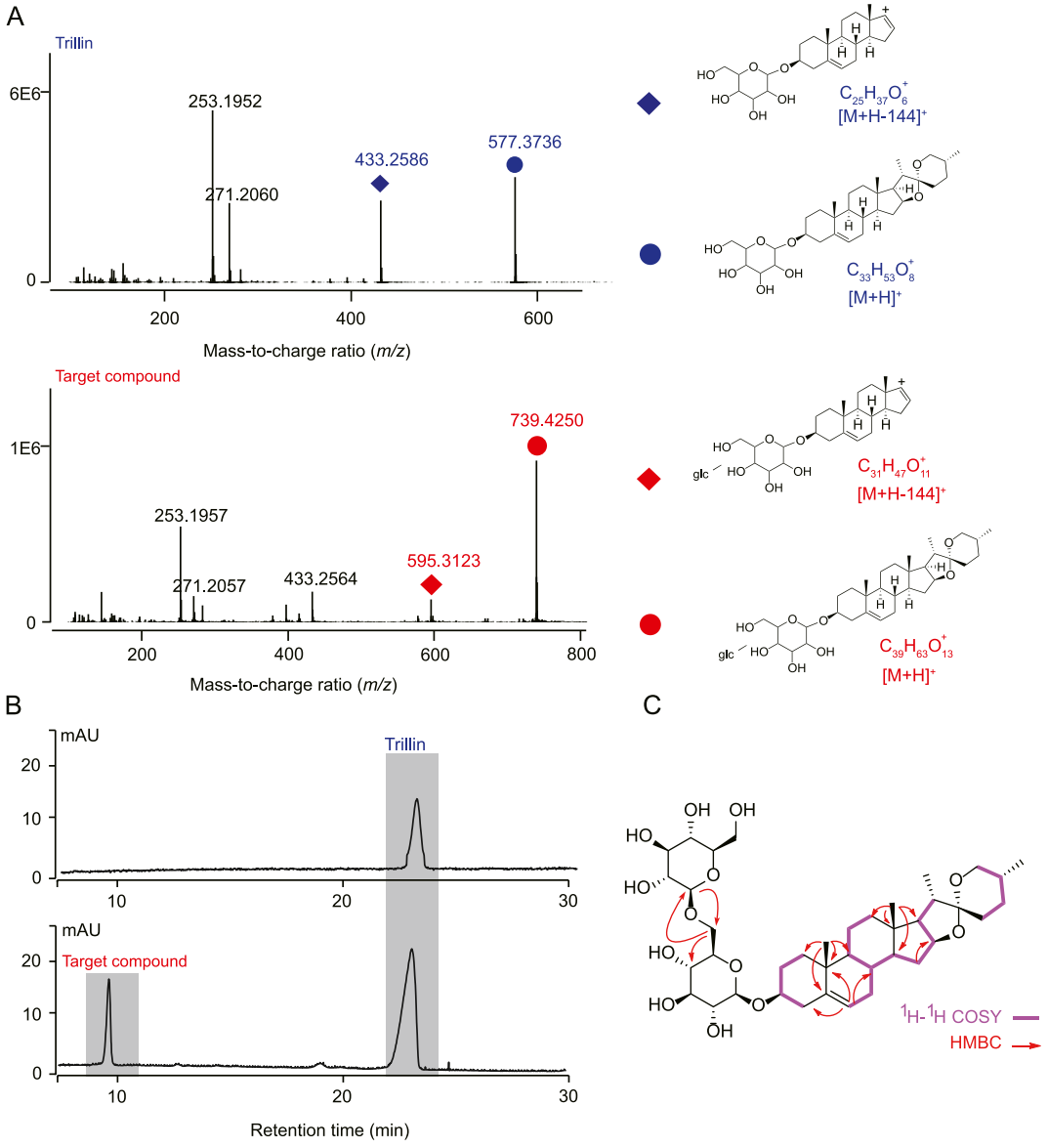

Fig. 2. Structural determination of the product produced by *Pp*UGT91AH4 and *Pp*UGT91AH5. (A) MS/MS fragmentation pattern of trillin and its glycosylated product. (B) Preparative LC analysis of the new product. (C) 2D NMR analysis of the new product.

patterns between the new product and trillin identified shared daughter ions, including *m/z* 595.3123, 433.2564, and 271.2053, confirming that they possess similar backbone structures, with the new product differing only by the addition of a glucose moiety (Fig. 2A).

Since LC-MS analysis could not determine the specific position of the glucose moiety added to trillin (Fig. 2B), we proceeded to elucidate its structure using NMR. To this end, 30 mg of the new product was purified from enzymatic reactions and analyzed by ^{1}H and ^{13}C NMR spectroscopy (Supplementary Fig. S4 and Fig. S5). The HMBC correlations confirmed glycosylation at the 6′ position (Fig. 2C). Therefore, the new product generated by *Pp*UGT91AH4 or *Pp*UGT91AH5 was indeed trillin 6′-*O*-glucoside, confirming their roles as trillin 6′-*O*-glucosyltransferases. Having determined the structure of purified trillin 6′-*O*-glucoside, we were able to use it as a standard to evaluate the content of trillin 6′-*O*-glucoside in the rhizomes of *P. polyphylla*. In the five-year-old *P. polyphylla* rhizomes we collected, the trillin 6′-*O*-glucoside content was measured at 2.12 μg/g, respectively (Supplementary Table S2). This is consistent with the previous report that trillin 6′-*O*-glucoside exists in low abundance [6].

3.3. Biochemical characterization of *PpUGT91AH4* and *PpUGT91AH5*

We next explored the biochemical properties of *Pp*UGT91AH4 and *Pp*UGT91AH5 *in vitro*. Using trillin (glucose acceptor) and UDP-glucose (glucose donor), the optimal temperature and pH of these two glucosyltransferases were accessed. Both *Pp*UGT91AH4 and *Pp*UGT91AH5 exhibited the highest catalytic efficiency at 37 °C and pH 8.0 (Fig. 3A). Under saturated UDP-glucose conditions, the K_m values of *Pp*UGT91AH4 and *Pp*UGT91AH5 for trillin were determined to be 5.67 ± 0.84 mM and 7.81 ± 1.2 mM, respectively (Fig. 3B and C). Correspondingly, the K_{cat}/K_m values for *Pp*UGT91AH4 and *Pp*UGT91AH5 were calculated as 16.2 ± 6.3 $\mu M^{-1}\ s^{-1}$ and 11.5 ± 2.1 $\mu M^{-1}\ s^{-1}$, respectively (Fig. 3B and C). These results indicate that *Pp*UGT91AH4 exhibits slightly higher catalytic efficiency and substrate affinity for trillin compared to *Pp*UGT91AH5. Additionally, we tested whether *Pp*UGT91AH4 and *Pp*UGT91AH5 could utilize other sugars like UDP-rhamnose and UDP-arabinose. Unlike when UDP-glucose was used as the donor, we did not detect any new trillin derived products (Supplementary Fig. S6).

3.4. Reconstitution of trillin 6′-*O*-glucoside synthesis in *N. benthamiana*

Since all the enzymes required for trillin 6′-*O*-glucoside were identified, we next sought to reconstitute its biosynthesis in *N. benthamiana*. *Pp*CYP450s, including *Pp*CYP90B27, *Pp*CYP90G4 and *Pp*CYP94D108, were selected to synthesize diosgenin. *Pp*UGT73CR1 was chosen as the trillin synthase from diosgenin. Because *Pp*UGT91AH4 outperformed *Pp*UGT91AH5 *in vitro*, *Pp*UGT91AH4 was selected as the last enzyme. The encoding genes were cloned into the pEAQ-HT-GFP and transformed into *A. tumefaciens*. The transformed *A. tumefaciens* strains were then mixed (1:1) and infiltrated into *N. benthamiana* leaves (Fig. 4).

Five days after the infiltration, the leaves were harvested for metabolic profiling. As expected, the biosynthesis of diosgenin or trillin was detected when the corresponding enzymes were co-infiltrated (Fig. 4). Building on this, the addition of *Pp*UGT91AH4 enabled the successful reconstitution of trillin 6′-*O*-glucoside in *N. benthamiana* leaves (Fig. 4). Thus, the heterologous production of trillin 6′-*O*-glucoside can be accomplished in *N. benthamiana* leaves within days, as opposed to the years required for its production in *P. polyphylla* rhizomes. Together, our results highlight the advantages of using biosynthetic methods to produce natural products that are present in low or trace abundances.

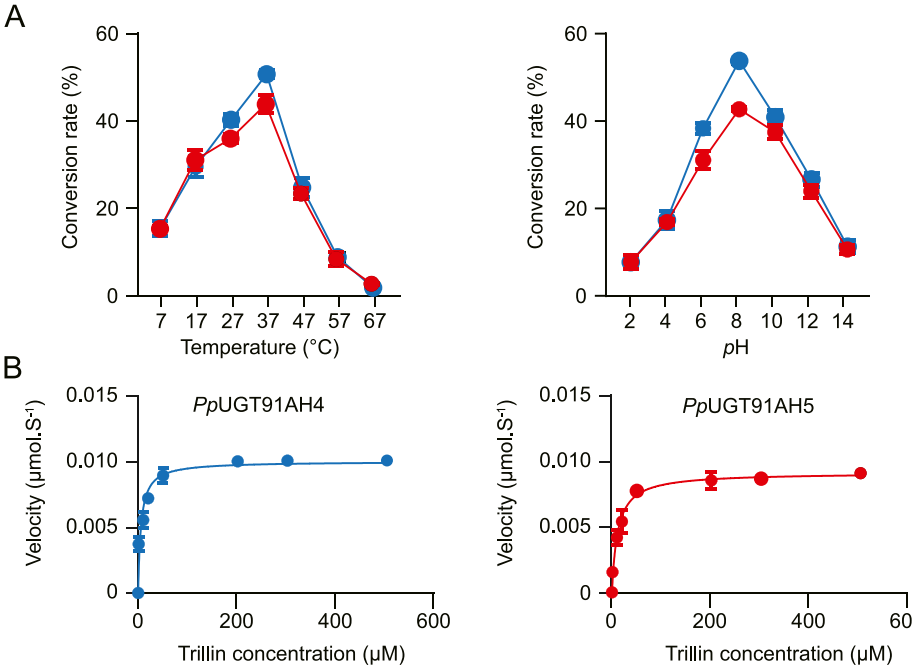

C

Substrate	Enzyme	K_m (mM)	K_{cat}/K_m ($\mu M^{-1}\ .S^{-1}$)
Trillin	*Pp*UGT91AH4	5.67 ± 0.84	16.2 ± 6.3
Trillin	*Pp*UGT91AH5	7.81 ± 1.2	11.5 ± 2.1

Fig. 3. Biochemical characterization of *Pp*UGT91AH4 and *Pp*UGT91AH5. (A) Optimal temperature and pH of *Pp*UGT91AH4 and *Pp*UGT91AH5. (B) Kinetic analysis of *Pp*UGT91AH4 and *Pp*UGT91AH5 using trillin as the substrate and UDP-glucose as the donor. Error bars represent standard deviation from triplicate assays. (C) K_m and K_{cat}/K_m of *Pp*UGT91AH4 and *Pp*UGT91AH5.

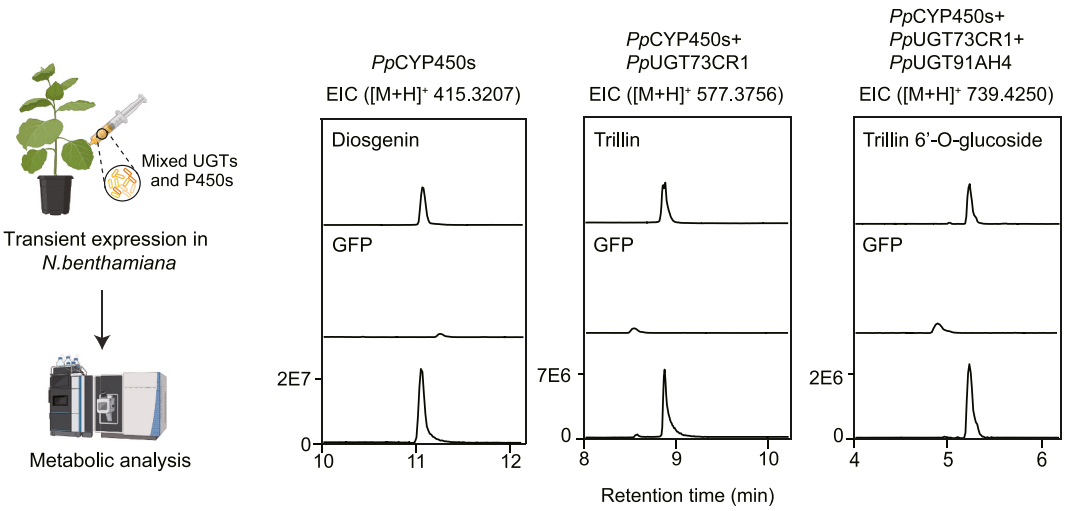

Fig. 4. Biosynthesis of trillin 6′-*O*-glucoside in *N. benthamiana*. Extracts from *N. benthamiana* leaves co-expressing *Pp*CYP450s, *Pp*CYP450s + *Pp*UGT73CR1, or *Pp*CYP450s + *Pp*UGT73CR1 + *Pp*UGT91AH4 are analyzed by LC-MS. The products were identified as $[M + H]^+$ ions.

3.5. Pharmacological activities of trillin 6′-O-glucoside

As we have produced sufficient amount of trillin 6′-*O*-glucoside, it enabled us to evaluate its pharmacological activities. Previous studies have clearly established the anti-bacteria activities of major polyphyllins, such as polyphyllins I, II, and VII. Could trillin 6′-*O*-glucoside also exhibit similar anti-bacteria activities?

To investigate this, we tested the potential inhibitory effects of trillin 6′-*O*-glucoside on five different bacteria species that can be associated with human infections, including three Gram-positive bacteria (*S. aureus*, *C. difficile*, and *P. anaerobius*) and two Gram-negative bacteria (*C. jejuni* and *V. parvula*). Anaerobic bacteria like *C. difficile*, *P. anaerobius*, and *V. parvula* were cultured in inverted plates placed within anaerobic bags. Neither diosgenin or trillin showed any detectable inhibitory effects against the five bacterial species at the concentration used (Fig. 5A). By contrast, trillin 6′-*O*-glucoside demonstrated inhibitory activities comparable to polyphyllins I, II, and VII, particularly against Gram-positive bacteria such as *S. aureus* and *P. anaerobius* (Fig. 5A). For Gram-negative bacteria like *C. jejuni* and *V. parvula*, the inhibitory effects of trillin 6′-*O*-glucoside were milder but still significant and comparable to polyphyllin VII (Fig. 5A). Using *S. aureus* as an example, we performed scanning electron microscopy analysis and found that the treatment of trillin 6′-*O*-glucoside disrupted bacterial cell structures (Supplementary Fig. S7). Thus, despite its relatively simple chemical structure, trillin 6′-*O*-glucoside displayed similar anti-bacterial activities on par with the more structurally complex major polyphyllins. It will be interesting to explore why trillin lacks anti-bacterial activities, while trillin 6′-*O*-glucoside acquires the properties in future studies.

Previous studies have shown that the major polyphyllins, such as polyphyllins I, II, and VII, have a shared side effect—hemolytic activity [37]. Given that trillin 6′-*O*-glucoside demonstrated anti-bacterial activities comparable to those major polyphyllins, could it also exhibit similar hemolytic activity? To test this, we incubated different concentrations of polyphyllin I, polyphyllin II, polyphyllin VII, and trillin 6′-*O*-glucoside with erythrocytes to measure the hemolytic activity. The activity was quantified by the EC_{50} value, which represented the compound concentration required to induce 50 % hemolysis of erythrocytes. Remarkably, the EC_{50} of trillin 6′-*O*-glucoside was much higher than those of polyphyllins I, II, and VII (Fig. 5B). For instance, the EC_{50} of trillin 6′-*O*-glucoside was over 500-fold higher than that of polyphyllin VII (Fig. 5C).

Taken together, these results suggest that trillin 6′-*O*-glucoside may hold the promise to be an equally potent yet significantly safer polyphyllin for clinical applications.

4. Discussion

Natural products from medicinal plants have been an invaluable resource for drug discovery and development. The conventional process typically begins with the large-scale collection of wild medicinal plants, followed by the extraction of natural products using appropriate solvents [38,39]. The extracts are then fractionated and purified into relatively pure compounds using various chromatographic methods. Finally, the biological activity of these compounds, obtained in sufficient quantities, is evaluated through cell-based assays or animal studies to identify potential lead molecules. Over the years, a vast amount of information on the chemical diversity of medicinal plants has been documented [40,41]. It is important to note that a significant portion of this diversity comprise natural products that occur in low or trace amounts within their native plants [42]. Despite their prevalence, these compounds largely unexplored due to the challenge of obtaining sufficient quantities for functional studies. Even though chemical synthesis represents a theoretically feasible route, synthesizing and purifying natural products with complicated stereochemistry and/or functional groups can be lab-intensive and technically challenging. Fortunately, the advent of synthetic biology offers a solution to obtain these natural products with low or trace amounts [43].

In this study, we used trillin 6′-*O*-glucoside as an example to illustrate how biosynthetic approaches are adept at exploring low-abundance natural products with significant pharmacological potential. We chose to focus on trillin 6′-*O*-glucoside because it is a low-abundance polyphyllin derived from *P. polyphylla*, a medicinally important plant. Interestingly, chemically synthesized trillin 6′-*O*-glucoside exhibits antifungal activities [28]. *P. polyphylla* has a long history of use in Chinese traditional medicine and has been extensively studied in the field of natural product chemistry [44]. Through this work, we aim to demonstrate that even well-studied medicinal plants like *P. polyphylla* can be revisited to explore their low-abundance compounds, unlocking the full potential of their chemical diversity using the biosynthetic approaches. The chemical structure of trillin 6′-*O*-glucoside suggests that its biosynthesis likely involves two glycosyltransferases, starting from diosgenin and proceeding through trillin as the mono-glycosylated intermediate. Building on previous studies of steroidal saponin biosynthesis, the key challenge in elucidating the biosynthetic pathway of trillin 6′-*O*-glucoside was identifying the second glycosyltransferase, which had yet to be discovered.

Using an *in vitro* enzyme assay, we identified two glucosyltransferases that used UDP-glucose as the sugar donor to modify trillin and synthesize a new, more hydrophilic product. We purified the new

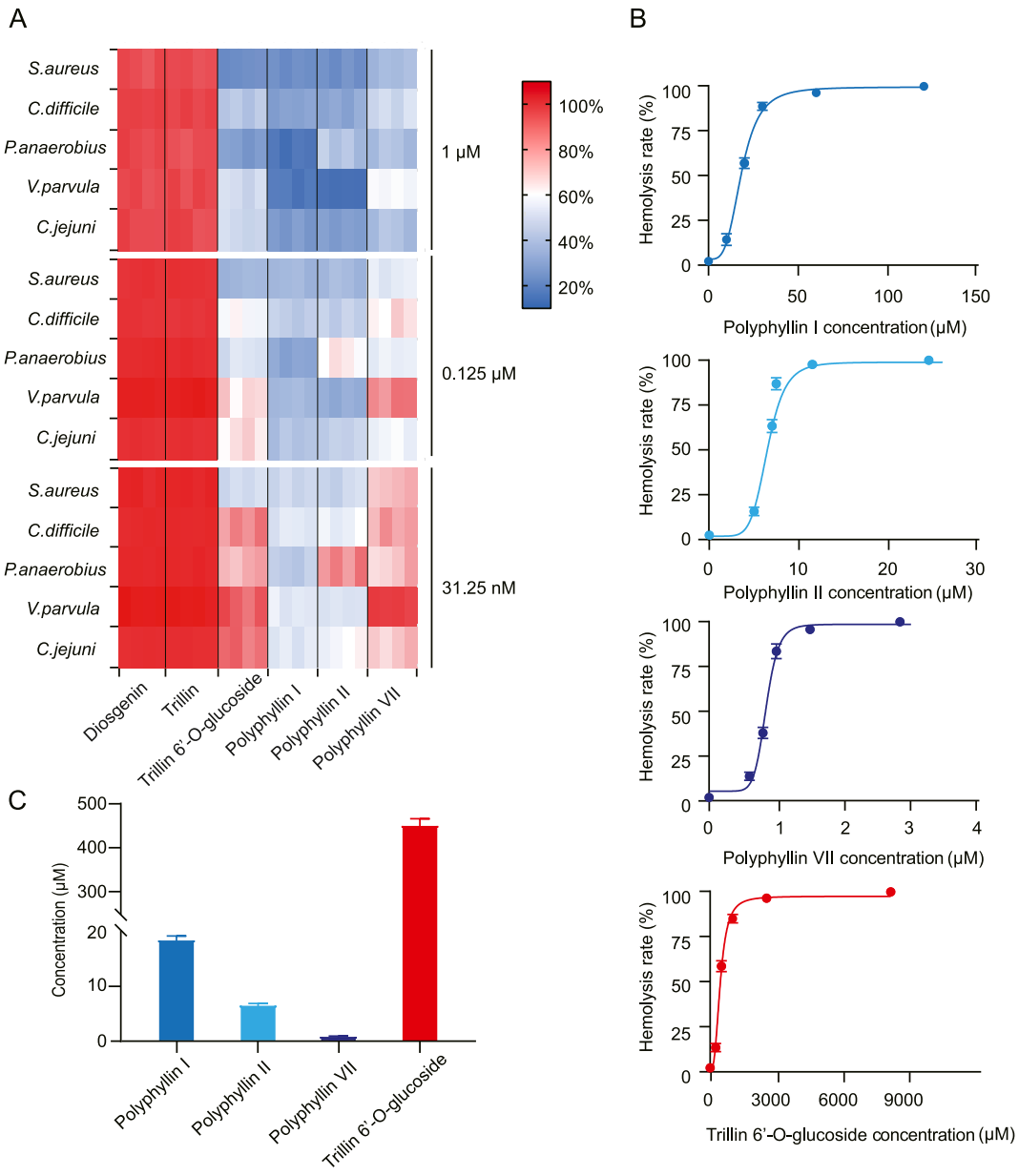

Fig. 5. Pharmacological activities of trillin 6′-*O*-glucoside. (A) Heatmap illustrating the anti-bacterial activities polyphyllin I, II, VII, trillin 6′-*O*-glucoside, trillin, and diosgenin at various concentrations. Bacterial survival rates are assayed in quadruplicate and represented in color gradient. (B) Hemolytic rate curves for polyphyllin I, II, VII, and trillin 6′-*O*-glucoside. (C) Concentrations of polyphyllin I, II, VII and trillin 6′-*O*-glucoside required to induce 50 % hemolysis.

compound and confirmed its identity as trillin 6′-*O*-glucoside through NMR analysis. This finding established that the two glucosyltransferases function as trillin 6′-*O*-glucosyltransferases. Phylogenetic analysis classified them within the UGT91 subfamily, which aligns with their biochemical functions, as other members of this subfamily are also characterized as steroid 6′-*O*-glucosyltransferases. Accordingly, we designated these enzymes as *Pp*UGT91AH4 and *Pp*UGT91AH5. Biochemical analysis revealed that *Pp*UGT91AH4 and *Pp*UGT91AH5 exhibited catalytic efficiency comparable to other reported *Pp*UGTs. Therefore, the low abundance of trillin 6′-*O*-glucoside in *P. polyphylla* is likely due to their limited access to substrates. The identification of the final enzyme in the biosynthesis of trillin 6′-*O*-glucoside, combined with the previously discovered enzymes, allowed us to reconstruct the entire pathway in *N. benthamiana* leaves. It is important to note that these transient expression experiments are intended as a proof-of-concept. Future studies should consider developing transgenic plants with stable expression of the biosynthetic genes.

Since we could produce sufficient amount of trillin 6′-*O*-glucoside, we also evaluate its pharmacological activities. The trillin 6′-*O*-glucoside used in the pharmacological studies was generated through enzymatic reactions. It should be noted that both chassis-based synthesis of natural products and *in vitro* enzymatic reactions are equally important for production. The choice between these approaches should depend on which one is more feasible for the specific context. Due to the scope limitations of this study, we focused on two key aspects of polyphyllins: their well-established antibacterial activity and their hemolytic effects, which are a recognized side effect [35]. The tested bacterial species included both Gram-positive and Gram-negative bacteria, as well as anaerobic and aerobic strains. Interestingly, trillin 6′-*O*-glucoside displayed inhibitory activities comparable to polyphyllins I, II, and VII, particularly against Gram-positive bacteria. Moreover, unlike polyphyllins I, II, and VII, trillin 6′-*O*-glucoside had a much lower hemolytic activity. Thus, trillin 6′-*O*-glucoside has the potential to be an effective polyphyllin with similar potency but markedly reduced toxicity,

positioning it as a promising option for clinical applications.

5. Conclusion and future perspectives

In summary, we utilized biosynthetic approaches to produce trillin 6′-*O*-glucoside, a polyphyllin present only in trace amounts in *P. polyphylla* rhizomes. By obtaining sufficient quantities of trillin 6′-*O*-glucoside, we demonstrated that it exhibits antibacterial activity comparable to major polyphyllins while displaying significantly reduced hemolytic activity. This study underscores the potential of biosynthetic strategies to explore natural products that, despite their low abundance, possess equally significant pharmacological properties. We are confident that similar approaches can be applied to investigate other low-abundance natural products, potentially paving the way for the discovery of novel therapeutic agents.

CRediT authorship contribution statement

Yaran Suo: Methodology. **Shuyu Li:** Methodology, Conceptualization. **Haining Lyu:** Methodology, Funding acquisition. **Xin Zhao:** Methodology. **Jiale Xing:** Methodology. **Xin Chai:** Methodology. **Qian Zhang:** Methodology. **Chunjin Fu:** Methodology. **Chengchao Xu:** Writing – original draft, Supervision, Project administration, Funding acquisition. **Jingjing Liao:** Writing – review & editing, Methodology, Funding acquisition, Conceptualization.

Declaration of competing interest

The authors declare that they have no known competing financial interests or personal relationships that could have appeared to influence the work reported in this paper.

Acknowledgments

This work was supported by the National Key Research and Development Program of China (2020YFA0908000), CAMS Innovation Fund (CI2023E002, CI2021A05101, CI2021B014, CI2021A05104 and CI2023E005TS06), Scientific and technological innovation project of China Academy of Chinese Medical Sciences (CI2023D008) and Fundamental Research Funds for the Central Public Welfare Research Institutes (ZZ14-YQ-051, ZZ14-YQ-052, ZZ17-YQ-047, ZZ15-ND-10, ZZ16-ND-10-12, ZZ17-ND-10-02, ZZ17-ND-10-16 and ZZ16-XRZ-103). Additionally, cartoons in Fig. 4 and 1C were created with BioRender.com.

Appendix A. Supplementary data

Supplementary data to this article can be found online at https://doi.org/10.1016/j.synbio.2025.02.013.

References

[1] Ding YG, Zhao YL, Zhang J, Zuo ZT, Zhang QZ, Wang YZ. The traditional uses, phytochemistry, and pharmacological properties of *Paris* L. (Liliaceae): a review. J Ethnopharmacol 2021;278:114293. https://doi.org/10.1016/j.jep.2021.114293.
[2] Rawat JM, Pandey S, Rawat B, Rai N, Preeti P, Thakur A, et al. Traditional uses, active ingredients, and biological activities of *Paris polyphylla* Smith: a comprehensive review of an important Himalayan medicinal plant. J Chem 2023; 2023:1–18. https://doi.org/10.1155/2023/7947224.
[3] Qin XJ, Yu MY, Ni W, Yan H, Chen CX, Cheng YC, et al. Steroidal saponins from stems and leaves of *Paris polyphylla* var. *yunnanensis*. Phytochemistry 2016;121: 20–9. https://doi.org/10.1016/j.phytochem.2015.10.008.
[4] Wei JC, Gao WY, Yan XD, Wang Y, Jing SS, Xiao PG. Chemical constituents of plants from the genus *Paris*. Chem Biodivers 2014;11:1277–96. https://doi.org/10.1002/cbdv.201300083.
[5] Dan A, Hu Y, Chen R, Lin X, Tian Y, Wang S. Advances in research on chemical constituents and pharmacological effects of *Paecilomyces hepiali*. Food Sci Hum Wellness 2021;10:401–7. https://doi.org/10.1016/j.fshw.2021.04.002.
[6] Wu X, Wang L, Wang GC, Wang H, Dai Y, Ye WC, et al. New steroidal saponins and sterol glycosides from *Paris polyphylla* var. *yunnanensis*. Planta Med 2012;78: 1667–75. https://doi.org/10.1055/s-0032-1315239.
[7] Thakur U, Shashni S, Thakur N, Rana SK, Singh A. A review on *Paris polyphylla* Smith: a vulnerable medicinal plant species of a global significance. J Appl Res Med Aromat Plants 2023;33:100447. https://doi.org/10.1016/j.jarmap.2022.100447.
[8] Pu X, Ren J, Ma X, Liu L, Yu S, Li X, et al. Polyphylla saponin I has antiviral activity against influenza A virus. Int J Clin Exp Med 2015;8:18963–71.
[9] Zhang Y, Zhang J, Sun J, Zhang M, Liu X, Yang L, et al. Polyphyllin I, a strong antifungal compound against *Candida albicans*. Apmis 2023;131:626–35. https://doi.org/10.1111/apm.13353.
[10] Liu W, Chai Y, Hu L, Wang J, Pan X, Yuan H, et al. Polyphyllin VI induces apoptosis and autophagy via reactive oxygen species mediated JNK and P38 activation in glioma. OncoTargets Ther 2020;13:2275–88. https://doi.org/10.2147/OTT.S243953.
[11] Tian Y, Gong GY, Ma LL, Wang ZQ, Song D, Fang MY. Anti-cancer effects of polyphyllin I: an update in 5 years. Chem Biol Interact 2020;316:108936. https://doi.org/10.1016/j.cbi.2019.108936.
[12] Niu W, Xu L, Li J, Zhai Y, Sun Z, Shi W, et al. Polyphyllin II inhibits human bladder cancer migration and invasion by regulating EMT-associated factors and MMPs. Oncol Lett 2020;20:2928–36. https://doi.org/10.3892/ol.2020.11839.
[13] Kong M, Fan J, Dong A, Cheng H, Xu R. Effects of polyphyllin I on growth inhibition of human non-small lung cancer cells and in xenograft. Acta Biochim Biophys Sin 2010;42:827–33. https://doi.org/10.1093/abbs/gmq091.
[14] Shan L, Chen Y, An G, Tao X, Qiao C, Chen M, et al. Polyphyllin I exerts anti-hepatocellular carcinoma activity by targeting ZBTB16 to activate the PPARγ/RXRα signaling pathway. Chin Med 2024;19:1–17. https://doi.org/10.1186/s13020-024-00984-0.
[15] Li L, Chen Z, Hao C. Neuroprotective effects of polyphyllin VI against rotenone-induced toxicity in SH-SY5Y cells. Brain Res 2024;1830:148824. https://doi.org/10.1016/j.brainres.2024.148824.
[16] Zhang Z, Wang T, Luo Z, Zaib MH, Yi M, Zeng H, et al. Anti-inflammatory and analgesic properties of polyphyllin VI revealed by network pharmacology and RNA sequencing. Purinergic Signal 2024;20:449–63. https://doi.org/10.1007/s11302-023-09979-2.
[17] Weber J, Schwarz M, Schiefer A, Hametner C, Häubl G, Fröhlich J, et al. Chemical Glucosylation of labile natural products using a (2-nitrophenyl) acetyl-protected glucosyl acetimidate donor. Eur J Org Chem 2018;2018:2701–6. https://doi.org/10.1002/ejoc.201800260.
[18] Romanowski S, Eustáquio AS. Synthetic biology for natural product drug production and engineering. Curr Opin Chem Biol 2020;58:137–45. https://doi.org/10.1016/j.cbpa.2020.09.006.
[19] Yin X, Liu J, Kou C, Lu J, Zhang H, Song W, et al. Deciphering the network of cholesterol biosynthesis in *Paris polyphylla* laid a base for efficient diosgenin production in plant chassis. Metab Eng 2023;76:232–46. https://doi.org/10.1016/j.ymben.2023.02.009.
[20] Christ B, Xu C, Xu M, Li FS, Wada N, Mitchell AJ, et al. Repeated evolution of cytochrome P450-mediated spiroketal steroid biosynthesis in plants. Nat Commun 2019;10:1–11. https://doi.org/10.1038/s41467-019-11286-7.
[21] Zhou C, Yang Y, Tian J, Wu Y, An F, Li CZY. 22R- but not 22S-hydroxycholesterol is recruited for diosgenin biosynthesis. Plant J 2022;109:940–51. https://doi.org/10.1111/tpj.15604.
[22] Yin Y, Gao L, Zhang X, Gao W. A cytochrome P450 monooxygenase responsible for the C-22 hydroxylation step in the *Paris polyphylla* steroidal saponin biosynthesis pathway. Phytochemistry 2018;156:116–23. https://doi.org/10.1016/j.phytochem.2018.09.005.
[23] Hua X, Song W, Wang K, Yin X, Hao C, Duan B, et al. Effective prediction of biosynthetic pathway genes involved in bioactive polyphyllins in *Paris polyphylla*. Commun Biol 2022;5:50. https://doi.org/10.1038/s42003-022-03000-z.
[24] Song W, Zhang C, Wu J, Qi J, Hua X, Kang L, et al. Characterization of three *Paris Polyphylla* glycosyltransferases from different UGT families for steroid functionalization. ACS Synth Biol 2022;11:1669–80. https://doi.org/10.1021/acssynbio.2c00103.
[25] Chen Y, Yan Q, Ji Y, Bai X, Li D, Mu R, et al. Unraveling the serial glycosylation in the biosynthesis of steroidal saponins in the medicinal plant *Paris polyphylla* and their antifungal action. Acta Pharm Sin B 2023;13:4638–54. https://doi.org/10.1016/j.apsb.2023.05.033.
[26] He M, Guo S, Yin Y, Zhang C, Zhang X. A novel sterol glycosyltransferase catalyses steroidal sapogenin 3-O glucosylation from *Paris polyphylla* var. *yunnanensis*. Mol Biol Rep 2023;50:2137–46. https://doi.org/10.1007/s11033-022-08199-y.
[27] Li J, Mosongo I, Li H, Wu Y, Li C, Yang S, et al. Identification and characterization of a trillin rhamnosyltransferase from *Dioscorea Zingiberensis*. Front Plant Sci 2021; 12:1–9. https://doi.org/10.3389/fpls.t.713036.
[28] Glennon RA, Dukat M. Structure-activity relationships of synthetic diosgenyl diglycosides. Phytochemistry 1992;31:3280–1. https://doi.org/10.1016/0031-9422(92)83496-L.
[29] Goulet MC, Gaudreau L, Gagné M, Maltais AM, Laliberté AC, Éthier G, et al. Production of biopharmaceuticals in *Nicotiana benthamiana*—axillary stem growth as a key determinant of total protein yield. Front Plant Sci 2019;10:735. https://doi.org/10.3389/fpls.2019.00735.
[30] Gao X, Su Q, Li J, Yang W, Yao B, Guo J, et al. RNA-Seq analysis reveals the important co-expressed genes associated with polyphyllin biosynthesis during the developmental stages of *Paris polyphylla*. BMC Genom 2022;23:1–17. https://doi.org/10.1186/s12864-022-08792-2.

[31] Chen C, Wu Y, Li J, Wang X, Zeng Z, Xu J, et al. TBtools-II: a "one for all, all for one" bioinformatics platform for biological big-data mining. Mol Plant 2023;16:1733–42. https://doi.org/10.1016/j.molp.2023.09.010.
[32] Li S, Chen S, Fu C, Zhang J, Xing J, Chai X, Zhang Q, Zhou J, Lyu H, Xu CLJ. Identification and characterization of *Pp*UGT91BP1 as a trillin synthase from *Paris polyphylla*. Plant Cell Physiol 2025;66:249–259. https://doi.org/10.1093/pcp/pcae147. pcae147.
[33] Tsoi H, Chu ESH, Zhang X, Sheng J, Nakatsu G, Ng SC, et al. *Peptostreptococcus anaerobius* induces intracellular cholesterol biosynthesis in colon cells to induce proliferation and causes dysplasia in mice. Gastroenterology 2017;152:1419–1433.e5. https://doi.org/10.1053/j.gastro.2017.01.009.
[34] Jiang L, Ma Y, Xiong Y, Tan Y, Duan X, Liao X, et al. Ruthenium polypyridine complexes with triphenylamine groups as antibacterial agents against *Staphylococcus aureus* with membrane-disruptive mechanism. Front Chem 2022;10:1–16. https://doi.org/10.3389/fchem.2022.1035741.
[35] Liu Z, Li N, Gao W, Man S, Yin S, Liu C. Comparative study on hemostatic, cytotoxic and hemolytic activities of different species of *Paris* L. J Ethnopharmacol 2012;142:789–94. https://doi.org/10.1016/j.jep.2012.05.065.
[36] Gauthier C, Legault J, Girard-Lalancette K, Mshvildadze V, Pichette A. Haemolytic activity, cytotoxicity and membrane cell permeabilization of semi-synthetic and natural lupane- and oleanane-type saponins. Bioorg Med Chem 2009;17:2002–8. https://doi.org/10.1016/j.bmc.2009.01.022.
[37] Ning LH, Zhou B, Zhang YX, Li XP. Study on hemolytic mechanism of polyphyllin II. Zhongguo Zhongyao Zazhi 2015;40:3623–9. https://doi.org/10.4268/cjcmm20151820.
[38] Tian XL, Liu JZ, Jiang LJ, Kong WH, Fu YJ, Qin LP, et al. Efficient extraction and optimization procedures of polyphyllins from *Paris polyphylla* var *chinensis* by deep eutectic solvent coupled with ultrasonic-assisted extraction. Microchem J 2024;196:109692. https://doi.org/10.1016/j.microc.2023.109692.
[39] Liu JZ, Lin ZX, Kong WH, Zhang CC, Yuan Q, Fu YJ, et al. Ultrasonic-assisted extraction-synergistic deep eutectic solvents for green and efficient incremental extraction of *Paris polyphylla* saponins. J Mol Liq 2022;368:120644. https://doi.org/10.1016/j.molliq.2022.120644.
[40] Martinidou E, Palmieri L, Sordo M, Masuero D, Ourda M, Delucchi L, et al. Assessment of the chemical and genetic variability among accessions of *Cicerbita alpina* (L.) Wallr., an alpine plant with anthelmintic properties. Front Plant Sci 2023;14:1–17. https://doi.org/10.3389/fpls.2023.1269613.
[41] Tiwari D, Kewlani P, Gaira KS, Bhatt ID, Sundriyal RC, Pande V. Predicting phytochemical diversity of medicinal and aromatic plants (MAPs) across eco-climatic zones and elevation in uttarakhand using generalized additive model. Sci Rep 2023;13:1–11. https://doi.org/10.1038/s41598-023-37495-1.
[42] Fan W, Fan L, Wang Z, Mei Y, Liu L, Li L, et al. Rare ginsenosides: a unique perspective of ginseng research. J Adv Res 2024;66:303–28. https://doi.org/10.1016/j.jare.2024.01.003.
[43] Foldi J, Connolly JA, Takano E, Breitling R. Synthetic biology of natural products engineering: recent advances across the Discover-Design-Build-Test-Learn cycle. ACS Synth Biol 2024;9:2684–92. https://doi.org/10.1021/acssynbio.4c00391.
[44] Jing S, Wang Y, Li X, Man S, Gao W. Chemical constituents and antitumor activity from *Paris polyphylla* Smith var. *yunnanensis*. Nat Prod Res 2017;31:660–6. https://doi.org/10.1080/14786419.2016.1219861.